



# Journal of Applied Sciences

ISSN 1812-5654

**science**  
alert

**ANSI***net*  
an open access publisher  
<http://ansinet.com>

## The Fracture Strength of Eutectic Composite Ceramic Containing Lamellar Inclusion

Xinhua Ni, Cheng Chen, Yingchen Ma and Shuqin Zhang

Department of Basic Course, Mechanical Engineering College, Shijiazhuang, 050003, China

---

**Abstract:** Eutectic composite ceramic containing lamellar inclusion possessed good strengths at room temperature and high temperature. Firstly, under the conditions that the matrix, interphase and the lamellar inclusions are isotropic, the size dependent micromechanical stress field of the composites can be achieved. Then, stress concentration generated by the dislocation pile-up in interphase was analyzed and the maximum stress in the matrix was obtained. When the maximum stress is equal to the breaking strength of the matrix in molecular theory, the ultimate shear stress of the composites can be derived. Finally, the analytic expression of the eutectic composite ceramics can be obtained based on the relationship between shear stress and the load. The result shows that the fracture strength of such composite ceramics had obvious size dependence.

**Key words:** Eutectic composite ceramic, lamellar inclusion, micromechanical stress field, fracture strength, size dependence

---

### INTRODUCTION

The special micro-structure of the eutectic composite ceramics makes its mechanical property better compared with any single component in the material (Farmer and Sayir, 2002; Brewer *et al.*, 2004; LLorca and Orera, 2005). That is because heterogeneous interfaces exist in the eutectic composites. Heteroatom's segregate in the heterogeneous interface which changes the cell's composition of atom effectively and also lower the free energy of the interface. Since the eutectic phases share an identical oxygen iron surface, those heterogeneous interfaces distributed on the eutectic structure have covalent character, so the two phases can keep strong and stable electrostatic bond. Experimental studies indicate that the microstructure of  $\text{Al}_2\text{O}_3\text{-ZrO}_2$  ( $\text{Y}_2\text{O}_3$ ) ceramic composites and the orientation relationship between two eutectic phases are decided by material composition and the growth rate of crystal. Adding small amount of  $\text{Y}_2\text{O}_3$  with a lower growth rate, the eutectic structure is two-phase lamellar structure. Under the scanning rate of 20 mm/h, with 12 mol% Y added, the material is eutectic composite with lamellar  $\text{ZrO}_2$  distributed on  $\text{Al}_2\text{O}_3$ -matrix. Such material's performance is quite well: At room temperature, its strength has already reached 1.6 Gpa and its hardness reached  $18.5 \pm 0.2$  Gpa. Moreover, such mechanical property reduced quite little when the temperature is higher than  $1500^\circ\text{C}$ . It is strong constraint effects of interfaces between lamellar inclusions and the matrix that contribute to the superior performance. The failure of composite is a micro-mechanical damage evolution process, so its

mechanical property is closely related to the microstructure and fracture feature of composite.

In recent years, the composite gained notable progress on synthetic method, mechanical property and microscopic structure research. Some failure criterions for composite have been developed. A simple mathematical model for predicting the crushing stress of composite materials was derived and presented by Goh *et al.* (2008). Las and Zemcik (2008) focused on the numerical simulation of damage and fracture of unidirectional fiber-reinforced composite structure using the finite element method. The macro mechanical strength model of fiber eutectics and transformation particles composite ceramic was built by considering random orientation and length of fiber eutectics and the stress concentration duo to the dislocation pileup on the fiber- matrix interface Ni *et al.* (2011a). The four-phase model was applied to study the damage of composite ceramic with partially debonding interphase and the result showed that the strength of composite was determined by the  $45^\circ$  orientation three phase cell and has obvious size dependence: the micromechanical strength would decrease when the particle diameter increased (Ni *et al.* 2011b). Considering the joint effect of transformation particle and partially debonding interphase, the mixed-mode I-II crack toughening model of transformation composite ceramic with partially debonding interphase is determined (Ni *et al.*, 2011c).

However, the study of micromechanics for eutectic ceramic composites with lamellar inclusions has not been reported in literature. In order to reveal the relationship between the macroscopically performance and the

microstructure of such composite ceramics, it is necessary to build corresponding micromechanical modal. Hence, this paper takes it as target and makes analysis of it. In this paper, four-phase modeling method was used to study the micromechanical stress field of such composite ceramics, based on which ,the maximum tensile stress of the material can be obtained by studying the stress concentration at two-phase interface. And when the max tensile stress is equal to the breaking strength in molecular theory, the ultimate shear stress of eutectic ceramics can be calculated. The last step is to work out the theoretical expression of material's fracture strength, on the base of the relationship between shear stress and load in the matrix.

**THE MICROMECHANICAL STRESS FIELD**

The lamellar inclusion with the strong constraining interphase is called two-phase cell; firstly, the two-phase cell is set in a finite matrix material region which is called matrix atmosphere, the two-phase cell with the matrix atmosphere has the name of three-phase cell; then we put the three-phase cell in the infinite effective medium that has the same elastic property with eutectic composite ceramic; the lamellar inclusion, interphase, matrix and effective medium together tend to form four-phase model, shown in Fig. 1. The volume fractions of every phase in the three-phase cell are same with the ones in the eutectic composite ceramic; all of lamellar inclusions have the same direction. Considerably, all of three-phase cells have the same shape and trait, so we only choose a three-phase cell to analyze.

Letting  $C, C_0, C_p$  and  $C_l$  are separately the stiffness tensor of the effective medium, matrix, interphase and lamellar inclusion and  $S, S_0, S_p$  and  $S_l$  are separately compliance tensor of the effective medium, matrix, interphase and lamellar inclusion. The compliance tensor increment of effective medium can be expressed:

$$H = S - S_0 \tag{1}$$

Obviously the compliance waves of interphase and lamellar inclusion are separately as follows:

$$H_l = S_l - S_0 \tag{2}$$

$$H_p = S_p - S_0 \tag{3}$$

Apparently, if we want to determinate the mechanical stress field in the three-phase cell, the flexibility tensor of effective medium has to be estimated. After considering

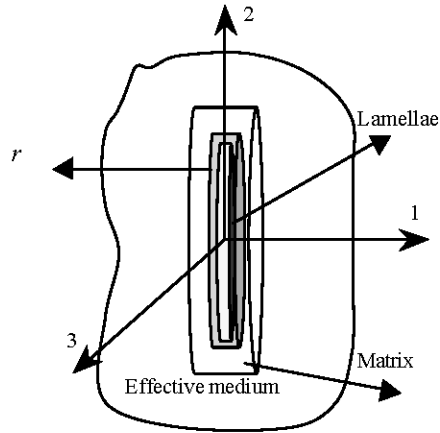


Fig. 1: The four-phase model of eutectic composite ceramic

the interphase, according to Eshelby sparse solutions we can know the mean strain tensor, as follow:

$$\bar{\epsilon} = S_0 \sigma_\infty + \sum (f_l H_l \sigma_l + f_p H_p \sigma_p) \tag{4}$$

where,  $f_p$  and  $f_l$  separately stands for the volume fraction of the interphase and lamellar inclusion.  $\sigma_\infty, \sigma_p$  and  $\sigma_l$  are separately the stress tensor in far field, the average stress tensors of the interphase and lamellar inclusion. The effective compliance tensor  $S$  that we definite it from the equivalent stress formula  $\bar{\epsilon} = S \sigma_\infty$  need to meet the relation:

$$H \sigma_\infty = \sum (f_l H_l \sigma_l + f_p H_p \sigma_p) \tag{5}$$

According to four-phase model method (Li *et al.*, 2011), we can recognize the equivalent stress tensor of the matrix, interphase and lamellar inclusion in the three-phase cell as follows:

$$\sigma_0 = (I - \Omega H)^{-1} \sigma^\infty \tag{6}$$

$$\sigma_p = (I + \Omega H_p)^{-1} \sigma_0 \tag{7}$$

$$\sigma_l = (I + \Omega H_l)^{-1} \sigma_0 \tag{8}$$

Therein,  $\Omega = C_0(I - M)$ ,  $I$  is the unit tensor,  $M$  corresponds to Eshelby tensor of lamellar inclusions. We substitute formula (7) and (8) into (5), after simplification, we can get a formula about compliance tensor increment  $H$  as follow:

$$H = (I - \sum H^d \Omega)^{-1} H^d \tag{9}$$

Where:

$$H^d = \sum [f_p(H_p^{-1} + \Omega)^{-1} + f_i(H_i^{-1} + \Omega)^{-1}] \quad (10)$$

Substituting formula (10) into (6), the stress tensor of the matrix can be determined. The results indicate that the stress field in the eutectic composite ceramic is associated with the stiffness and the volume fractions of each component in the eutectic composite ceramic, the shape of lamellar inclusion. If the elastic constants of the matrix, interphase and inclusion have been known, we could make a quantitative analysis on the stresses of the matrix. Hypothetically, coordinate axis 1 is perpendicular to the lamellar inclusion, coordinate axes 2 and 3 parallel to the lamellar inclusion. If the eutectic composite ceramic is suffered from the tension stress  $\sigma_\infty$  along coordinate axis 2, we get the dimensionless components of the stress tensor in the matrix:

$$\frac{\sigma_{11}^0}{\sigma_\infty^0}, \frac{\sigma_{22}^0}{\sigma_\infty^0} \text{ and } \frac{\sigma_{33}^0}{\sigma_\infty^0}$$

$$\frac{\sigma_{11}^0}{\sigma_\infty^0} = \delta_{12}, \frac{\sigma_{22}^0}{\sigma_\infty^0} = \delta_{22}, \frac{\sigma_{33}^0}{\sigma_\infty^0} = \delta_{23} \quad (11)$$

where,  $\delta_{12}$ ,  $\delta_{22}$  and  $\delta_{23}$  are given in Appendix. In regard to  $Al_2O_3-ZrO_2$  eutectic composite ceramic,  $f_p = 2f_i\Delta/h$ ,  $\Delta$  is the thickness of interphase,  $h$  is the thickness of lamellar inclusion.  $\Delta$  is generally a constant, so the graphs of the normal stresses in the matrix, following the change of  $h$ , are charted as shown in Fig. 2-4, while the shearing stresses are zero.

From Fig. 2, when the thickness of the lamellar inclusion is smaller, the stress perpendicular to the lamellar inclusion is compressive, otherwise is tensile, the numeric of the stress decreases the thickness of the lamellar inclusion. As shown in Fig. 3, the stress which is along the direction of external load is tensile stress, such stress increases with the thickness of the lamellar inclusion and the larger the thickness is, the more smooth the numeric of tensile stress changes, the smaller the thickness is, the sharper its numeric varies.

As shown in Fig. 4, we can see that the stress which is parallel to the lamellar inclusion and perpendicular to the direction of external load is compressive, its numeric decreases with  $h$ , moreover, the larger the thickness of the lamellar inclusion is, the more smooth the numeric of compressive stress changes, on the contrary, the smaller the thickness of the lamellar inclusion is, the sharper its numeric varies.

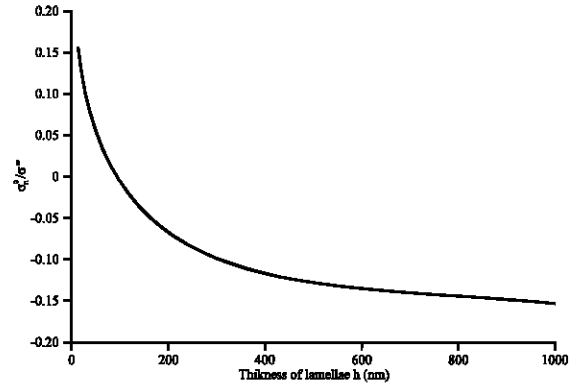


Fig. 2: Relation between the stress in matrix along the axis 1 and the thickness of lamellar inclusion

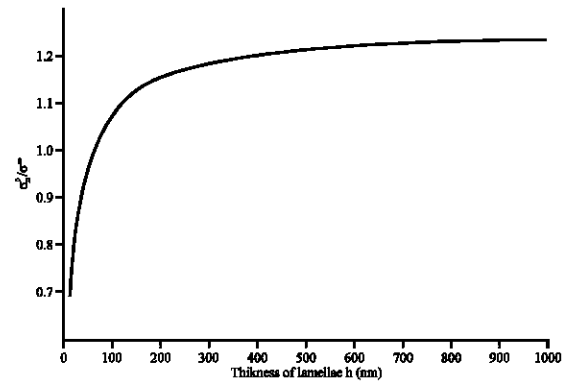


Fig. 3: Relation between the stress in matrix along the axis 2 and the thickness of lamellar inclusion

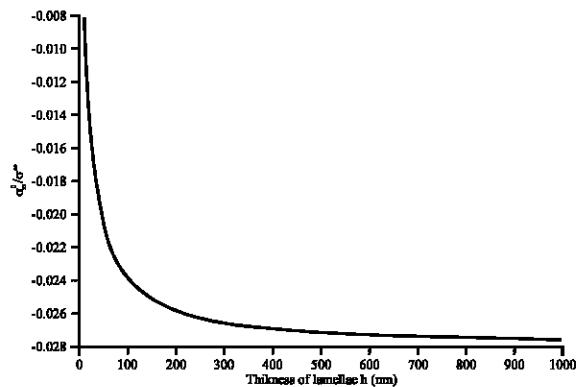


Fig. 4: Relation between the stress in matrix along the axis 3 and the thickness of lamellar inclusion

Synthetically, we can know from Fig. 2-4, the numeric of tensile stress along the direction of external load is maximal, the numeric of stress perpendicular to the lamellar inclusion is less, the stress parallel to the lamellar

inclusion and perpendicular to the direction of external load is minimum. So the tensile stress along the direction of external load is the main factor that causes damage. From variable tendency, we can see that the primal stress increases with the thickness of the lamellar inclusion, that is to say, the larger the thickness of the lamellar inclusion is and the higher the stress is also, the matrix is easier to destroy.

**THE MICRO STRENGTH OF EUTECTIC COMPOSITE CERAMIC**

There is not slippage system which can engender macroscopic plastic flow in the oxide ceramic, but there is microcosmic plastic deformation. This microcosmic plastic deformation is microcosmic heterogeneous plastic flow created by faintish glide system. Namely correspond to lowest frictional resistance of dislocation motion, it makes crack to nucleate and extend. Crystal lattice would glide and dislocation source are created around the lamellar inclusion due to external stress. And when the maximum shearing stress reaches a certain numerical value, dislocation source starts to let out dislocation. Under the effect of shearing stress, dislocations slip forwards and pile up the interphase, shown in Fig. 5.

Along with the increase of shearing stress, dislocation source lets out dislocation and moves forwards continually along the slip plane. Then dislocation pileup group forms at the interphase. Dislocation amount  $t$  in dislocation pileup group is related to the size of external shearing stress  $\tau$  and the length of slippage system, that can be described (Ni *et al.*, 2011 c)

$$t = \frac{k\pi h(\tau - \tau_i)}{\mu_0 b} \tag{12}$$

where,  $k$  is a constant that is related to the type of dislocation, to helix dislocation  $k = 1$  and edge dislocation  $k = 1 - \nu_0$ ,  $\nu_0$  is Poisson ratio of the matrix.  $h$  is the thickness

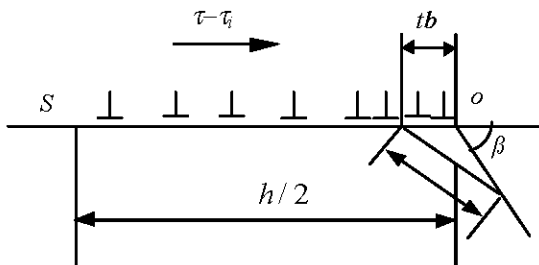


Fig. 5: The dislocation pile-up model

of the lamellar inclusion.  $\tau_i$  is resistance of crystal lattice against dislocation motion.  $b$  is Burgers vector.  $\mu_0$  is the shear modulus of the matrix.

Dislocation in dislocation pileup group is not uniformly distributed. The dislocation density is higher where is nearer the interphase. Resulting from dislocation pileup, there is a force acts on interphase. The numerical value of this force is  $t$  times to  $(\tau - \tau_i)$ . Frictional resistance of dislocation motion is tininess, so the force on interphase approximates  $t$  times to the shearing stress  $\tau$ . Owing to there is stress concentration between leading dislocation and the interphase, there is a stress field around the stress concentration. Hypothesize that there is a point at a distance  $r$  to leading dislocation, the maximum tensile stress perpendicular to  $r$  direction in  $P$  point that is aroused by the stress filed can be gotten:

$$\sigma_{max} = \frac{2}{\sqrt{3}} \left( \frac{h}{r} \right)^{\frac{1}{2}} (\tau - \tau_i) \tag{13}$$

The theoretic fracture strength of matrix is:

$$\sigma_{th} = \left( \frac{E_0 \gamma_0}{a_0} \right)^{\frac{1}{2}} \tag{14}$$

where,  $E_0$  and  $\gamma_0$  are the elastic modulus and free surface energy of matrix,  $a_0$  is lattice constant. Interphase in the eutectic is under the strong constraint of covalence, so it can not be destroyed. The matrix near interphase will fracture, that is destroyed in  $r = 2a_0$ . Letting  $\sigma_{max} = \sigma_{th}$  and overlooking the resistance  $\tau_i$  of crystal lattice against dislocation motion, according to Eq. 13 and 14, we get the ultimate shear stress:

$$\tau_u = \tau_i + \sqrt{\frac{3E_0 \gamma_0}{2h}} \tag{15}$$

From Eq. 7, we have obtained the maximal stress  $\sigma_{22}^0$  and the minimum stress  $\sigma_{33}^0$  under the tension load  $s_{\infty}$ . So the maximal shear stress can be gotten as follow:

$$\tau_{max}^0 = \frac{\sigma_{22}^0 - \sigma_{33}^0}{2} \tag{16}$$

when the maximal shear stress equal to the ultimate shear stress, the eutectic composite ceramic will destroy. From Eq. 11 and 12, we get the fracture strength of the composite ceramic:

$$\sigma_c = \frac{2}{\delta_{22} - \delta_{23}} \left( \tau_i + \sqrt{\frac{3E_0 \gamma_0}{2h}} \right) \tag{17}$$

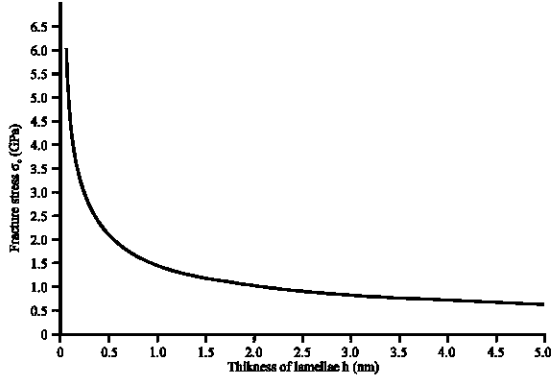


Fig. 6: Relation between the fracture strength and the thickness of lamellae

Overlooking the resistance  $\tau_i$  of crystal lattice against dislocation motion, the fracture strength of composite ceramic is given:

$$\sigma_c = \frac{1}{\delta_{22} - \delta_{23}} \sqrt{\frac{6E_0\gamma_0}{h}} \quad (18)$$

It revealed that the fracture strength of the eutectic composite ceramic containing lamellar inclusion would increase as the decrease of lamellae thickness  $h$ , as shown in Fig. 6. When  $h \leq 0.5 \mu\text{m}$ , there is a huge change range about the strength. This is because as the lamellae thickness is less, the distance between two interphase will be shorter and the total area of interphase will be more, then the strength will be higher; when  $h \geq 4 \mu\text{m}$ , the strength changed smoothly. When the thickness  $h$  increased to a certain extent, although the distance in interphase increased, the total area of interphase could not have more changes. So the curve of fracture strength changed smoothly.

### SUMMARY

Considering a fiber eutectic in composite ceramic having an orientation angle  $\theta$ , the micromechanical stress field of fiber-eutectic is determined. According to micromechanical stress field of fiber-eutectic, the micro fracture strength of the fiber-eutectic is gotten by calculating stress concentration created by the dislocation pile-up in the interphase. The macro strength model of the composite ceramics is built by the probabilities of ending fiber eutectics and bridging fiber eutectics. The macro strength of the composite ceramic is associated with the volume fraction, the elastic modulus and free surface energy of matrix in fiber eutectic. We pay attention to the size dependence of the macro strength: the fracture strength of the composite ceramic would increase as the decrease of fiber inclusion diameter. When

$d \leq 0.5 \mu\text{m}$ , there is a huge change range about the strength; when  $d \geq 4 \mu\text{m}$ , the strength changes smoothly. That indicates that nano-fiber in fiber-eutectics could make Fiber eutectics and transformation particles composite ceramic having high strength.

### ACKNOWLEDGMENTS

This study is supported by the National Natural Science Foundation of China under grant no. 11272355.

### APPENDIX

$$\begin{aligned} \delta_{12} &= \frac{\varpi_{12}}{(1-\varpi_{11})(1-\varpi_{22}-\varpi_{23})-2\varpi_{12}\varpi_{21}}, \\ \delta_{22} &= \frac{(1-\varpi_{11})(1-\varpi_{22})-\varpi_{12}\varpi_{21}}{(1-\varpi_{22}+\varpi_{23})\varpi}, \\ \delta_{23} &= \frac{(1-\varpi_{11})\varpi_{23}+\varpi_{12}\varpi_{21}}{(1-\varpi_{22}+\varpi_{23})\varpi}, \\ \varpi_{11} &= C_{11}^{\text{eff}}H_{1111}+2C_{12}^{\text{eff}}H_{2211}, \\ \varpi_{12} &= C_{11}^{\text{eff}}H_{1122}+C_{12}^{\text{eff}}(H_{2222}+H_{2233}), \\ \varpi_{21} &= C_{21}^{\text{eff}}H_{1111}+(C_{22}^{\text{eff}}+C_{23}^{\text{eff}})H_{2211}, \\ \varpi_{22} &= C_{21}^{\text{eff}}H_{1122}+C_{22}^{\text{eff}}H_{2222}+C_{23}^{\text{eff}}H_{2233}, \\ \varpi_{23} &= C_{21}^{\text{eff}}H_{1122}+C_{23}^{\text{eff}}H_{2222}+C_{22}^{\text{eff}}H_{2233} \\ C_{11}^{\text{eff}} &= K_0(1-M_{1111}-2M_{2211}) \\ &\quad +2\mu^*(1-M_{1111}+M_{2211}), \\ C_{12}^{\text{eff}} &= K_0(1-M_{2222}-M_{1122}-M_{2233}) \\ &\quad +\mu^*(M_{2233}+M_{2222}-2M_{1122}-1), \\ C_{21}^{\text{eff}} &= K_0(1-M_{1111}-2M_{2211}) \\ &\quad +\mu^*(M_{1111}-M_{2211}-1), \\ C_{22}^{\text{eff}} &= K_0(1-M_{2222}-M_{1122}-M_{2233}) \\ &\quad +\mu^*[2(1-M_{2222})+M_{1122}+M_{2233}], \\ C_{23}^{\text{eff}} &= K_0(1-M_{2222}-M_{1122}-M_{2233}) \\ &\quad +\mu^*(M_{1122}+M_{2222}-2M_{2233}-1) \\ H_{1111} &= \frac{h_{1111}}{E_0}, \quad H_{2222} = H_{3333} = \frac{h_{2222}}{E_0}, \\ H_{1122} &= H_{1133} = \frac{h_{1122}}{E_0}, \quad H_{2211} = H_{3311} = \frac{h_{2211}}{E_0}, \\ H_{1212} &= H_{1313} = \frac{h_{1212}}{\mu_0}, \quad H_{2323} = \frac{h_{2323}}{\mu_0} \\ h_{1111} &= \frac{J_{1111}(F_{2222}+F_{2233})-2F_{1122}J_{2211}}{F_{1111}(F_{2222}+F_{2233})-2F_{1122}F_{2211}}, \\ h_{2222} &= \frac{J_{22}-J_{23}-J_{12}}{(F_{2222}-F_{2233})(F_{1111}(F_{2222}+F_{2233})-2F_{1122}F_{2211})}, \\ J_{22} &= J_{2222}(F_{1111}F_{2222}-F_{1122}F_{2211}) \\ J_{23} &= J_{2233}(F_{1111}F_{2233}-F_{1122}F_{2211}) \\ J_{12} &= J_{1122}F_{2211}(F_{2222}-F_{2233}) \\ h_{1122} &= \frac{J_{1122}(F_{2222}+F_{2233})-F_{1122}(J_{2222}+J_{2233})}{F_{1111}(F_{2222}+F_{2233})-2F_{1122}F_{2211}}, \\ h_{2211} &= \frac{J_{2211}F_{1111}-J_{1111}F_{2211}}{F_{1111}(F_{2222}+F_{2233})-2F_{1122}F_{2211}}, \end{aligned}$$

$$h_{1212} = \frac{G_{1212}}{1 - G_{1212}(1 - 2M_{1212})},$$

$$h_{2323} = \frac{G_{2323}}{1 - G_{2323}(1 - 2M_{2323})},$$

$$G_{1212} = f_p(\mu_0 - \mu_p)/[\mu_p + (1 - 2M_{1212})(\mu_0 - \mu_p)] + f_l(\mu_0 - \mu_l)/[\mu_l + (1 - 2M_{1212})(\mu_0 - \mu_l)],$$

$$G_{2323} = f_p(\mu_0 - \mu_p)/[\mu_p + (1 - 2M_{2323})(\mu_0 - \mu_p)] + f_l(\mu_0 - \mu_l)/[\mu_l + (1 - 2M_{2323})(\mu_0 - \mu_l)],$$

$$J_{1111} = f_p(g_{22}^p + g_{23}^p)/[g_{11}^p(g_{22}^p + g_{23}^p) - 2g_{12}^p g_{21}^p] + f_l(g_{22}^l + g_{23}^l)/[g_{11}^l(g_{22}^l + g_{23}^l) - 2g_{12}^l g_{21}^l],$$

$$J_{1122} = -f_p g_{21}^p / [g_{11}^p(g_{22}^p + g_{23}^p) - 2g_{12}^p g_{21}^p] - f_l g_{21}^l / [g_{11}^l(g_{22}^l + g_{23}^l) - 2g_{12}^l g_{21}^l],$$

$$J_{2211} = -f_p g_{21}^p / [g_{11}^p(g_{22}^p + g_{23}^p) - 2g_{12}^p g_{21}^p] - f_l g_{21}^l / [g_{11}^l(g_{22}^l + g_{23}^l) - 2g_{12}^l g_{21}^l],$$

$$J_{2222} = f_p \frac{g_{11}^p g_{22}^p - g_{12}^p g_{21}^p}{(g_{22}^p - g_{23}^p)[g_{11}^p(g_{22}^p + g_{23}^p) - 2g_{12}^p g_{21}^p]} + f_l \frac{g_{11}^l g_{22}^l - g_{12}^l g_{21}^l}{(g_{22}^l - g_{23}^l)[g_{11}^l(g_{22}^l + g_{23}^l) - 2g_{12}^l g_{21}^l]},$$

$$J_{2233} = -f_p \frac{g_{11}^p g_{23}^p - g_{12}^p g_{21}^p}{(g_{22}^p - g_{23}^p)[g_{11}^p(g_{22}^p + g_{23}^p) - 2g_{12}^p g_{21}^p]} - f_l \frac{g_{11}^l g_{23}^l - g_{12}^l g_{21}^l}{(g_{22}^l - g_{23}^l)[g_{11}^l(g_{22}^l + g_{23}^l) - 2g_{12}^l g_{21}^l]},$$

$$F_{1111} = 1 - b_{11}, F_{1122} = -b_{12},$$

$$F_{2211} = -b_{21}, F_{2222} = 1 - b_{22}, F_{2233} = -b_{23},$$

$$b_{11} = J_{1111}Q_{11} + 2J_{1122}Q_{21},$$

$$b_{12} = J_{1111}Q_{12} + J_{1122}(Q_{22} + Q_{23}),$$

$$b_{21} = J_{2211}Q_{11} + Q_{21}(J_{2222} + J_{2233}),$$

$$b_{22} = J_{2211}Q_{12} + J_{2222}Q_{22} + J_{2233}Q_{23},$$

$$b_{23} = J_{2211}Q_{12} + J_{2222}Q_{23} + J_{2233}Q_{22},$$

$$Q_{11} = v_1^*(1 - M_{1111} - 2M_{2211}) + v_2^*(1 - M_{1111} + M_{2211}),$$

$$Q_{12} = v_1^*(1 - M_{1122} - M_{2222} - M_{2233}) + v_2^*(M_{2233} - 2M_{1122} + M_{2222} - 1),$$

$$Q_{21} = v_1^*(1 - M_{1111} - 2M_{2211}) + v_2^*(M_{1111} - M_{2211} - 1),$$

$$Q_{22} = v_1^*(1 - M_{1122} - M_{2222} - M_{2233}) + v_2^*[2(1 - M_{2222}) + M_{1122} + M_{2233}],$$

$$Q_{23} = v_1^*(1 - M_{1122} - M_{2222} - M_{2233}) + v_2^*(M_{1122} - M_{2233} + M_{2222} - 1),$$

$$g_{11}^p = v_1^*(p_k - M_{1111} - 2M_{2211}) + v_2^*(p_\mu - M_{1111} + M_{2211}),$$

$$g_{12}^p = v_1^*(p_k - M_{1122} - M_{2222} - M_{2233}) + v_2^*(M_{2233} - 2M_{1122} + M_{2222} - p_\mu),$$

$$g_{21}^p = v_1^*(p_k - M_{1111} - 2M_{2211}) + v_2^*(M_{1111} - M_{2211} - p_\mu),$$

$$g_{23}^p = v_1^*(p_k - M_{1122} - M_{2222} - M_{2233}) + v_2^*(M_{1122} - M_{2233} + M_{2222} - p_\mu),$$

$$g_{11}^l = v_1^*(l_k - M_{1111} - 2M_{2211}) + v_2^*(l_\mu - M_{1111} + M_{2211}),$$

$$g_{12}^l = v_1^*(l_k - M_{1122} - M_{2222} - M_{2233}) + v_2^*(M_{2233} - 2M_{1122} + M_{2222} - l_\mu),$$

$$g_{21}^l = v_1^*(l_k - M_{1111} - 2M_{2211}) + v_2^*(M_{1111} - M_{2211} - l_\mu),$$

$$g_{22}^l = v_1^*(l_k - M_{1122} - M_{2222} - M_{2233}) + v_2^*[2(1 - M_{2222}) + M_{1122} + M_{2233}],$$

$$g_{23}^l = v_1^*(l_k - M_{1122} - M_{2222} - M_{2233}) + v_2^*(M_{1122} - M_{2233} + M_{2222} - l_\mu),$$

$$p_k = \frac{K_0}{K_0 - K_p}, p_\mu = \frac{\mu_0}{\mu_0 - \mu_p},$$

$$l_k = \frac{K_0}{K_0 - K_l}, l_\mu = \frac{\mu_0}{\mu_0 - \mu_l}$$

$$v_1^* = \frac{1}{3(1 - 2\nu_0)}, v_2^* = \frac{1}{3(1 + 2\nu_0)}, \mu^* = \frac{2}{3}\mu_0$$

where,  $K_0$ ,  $K_p$  and  $K_l$  are the bulk modulus of matrix, interphase and lamellar inclusion,  $\mu_0$ ,  $\mu_p$  and  $\mu_l$  are shear modulus of matrix, interphase and lamellar inclusion.

## REFERENCES

- Brewer, L.N., M.U. Guruz and V.P. Dravid, 2004. Interfacial fracture mechanisms in solid solution directionally solidified eutectic oxide composites. *Acta Materialia*, 52: 3781-3791.
- Farmer, S.C. and A. Sayir, 2002. Tensile strength and microstructure of  $Al_2O_3$ -ZrO<sub>2</sub> Hypoeutectic fibers. *Eng. Fract. Mechanics*, 69: 1015-1024.
- Goh, S., H. Ku and S.L. Ang, 2008. Prediction of crushing stress in composite materials. *J. Composite Mater.*, 42: 467-484.
- Llorca, J. and V.M. Orera, 2005. Directionally solidified eutectic ceramic oxides. *Progress Mater. Sci.*, 51: 711-809.
- Las, V. and R. Zemcik, 2008. Progressive damage of unidirectional composite panels. *J. Composite Mater.*, 42: 25-44.
- Li, B.F., J. Zheng, X.H. Ni, Y.C. Ma and J. Zhang, 2011. Effective elastic constants of fiber-eutectics and transformation particles composite *Ceramic. Adv. Mater. Res.*, 177: 182-185.
- Ni, X.H., B.F. Li, Z. Zheng, X.Q. Liu, G.H. Zhong and L. Zhao, 2011a. Micromechanical strength of composite ceramic with partially debonding interphase. *Adv. Sci. Lett.*, 4: 1683-1686.
- Ni, X.H., T. Sun, X.Q. Liu, Q.H. Gu and X.F. Meng, 2011b. Size dependent strength of fiber eutectics and transformation particles composite ceramic. *Applied Mechanics Mater.*, 44-47: 2264-2268.
- Ni, X.H., X.Q. Liu, B.H. Han, S.Q. Zhang and Z.G. Cheng, 2011c. Size dependent fracture enhancement of transformation composite ceramic with partially debonding interphase. *Adv. Sci. Lett.*, 4: 1767-1770.